CORE
Metadata, citation and similar papers at core.ac.uk
Provided by Universiti Teknikal Malaysia Melaka: UTeM Open Journal System

EFFECT OF PULSE CURRENT MICRO PLASMA ARC WELDING PARAMETERS ON PITTING CORROSION RATE OF AISI 321 SHEETS IN 3.5 N NACL MEDIUM

Kondapalli Siva Prasad[1*], Chalamalasetti Srinivasa Rao[2]

[1*]Associate Professor, Department of Mechanical Engineering, Anil Neerukonda Institute of Technology & Sciences, Visakhapatnam, India

[2] Professor, Department of Mechanical Engineering, Andhra University, Visakhapatnam, India

ABSTRACT

Austenitic stainless steel sheets are used for fabrication of components, which require high temperature resistance and corrosion resistance such as metal bellows used in expansion joints in aircraft, aerospace and petroleum industries. When they are exposed to sea water after welding they are subjected to corrosion as there are changes in properties of the base metal after welding. The corrosion rate depends on the chemical composition of the base metal and the nature of welding process adopted. Corrosion resistance of welded joints can be improved by controlling the process parameters of the welding process. In the present work Pulsed Current Micro Plasma Arc Welding (MPAW) is carried out on AISI 321 austenitic stainless steel of 0.3 mm thick. Peak current, Base current, Pulse rate and Pulse width are chosen as the input parameters and pitting corrosion rate of weldment in 3.5N NaCl solution is considered as output response. Pitting corrosion rate is computed using Linear Polarization method from Tafel plots. Response Surface Method (RSM) is adopted by using Box-Behnken Design and total 27 experiments are performed. Empirical relation between input and output response is developed using statistical software and its adequacy is checked using Analysis of Variance (ANOVA) at 95% confidence level. The main effect and interaction effect of input parameters on output response are also studied.

KEYWORDS: *Plasma Arc Welding; Austentic Stainless Steel; Pitting Corrosion Rate*

1.0 INTRODUCTION

Austenitic Stainless Steel (ASS), being the widest in use of all the stainless steel groups finds application in the beverages industry, petrochemical, petroleum, food processing and textile industries amongst others. It has good tensile strength, impact resistance and wear resistance properties. In addition, it combines these with excellent corrosion resistant properties (Dillon, C. P., 1994).

* Corresponding author: kspanits@gmail.com

Welding is one of the most employed methods of fabricating ASS components. ASS is largely highly weldable; the higher the carbon content, the harder the SS and so the more difficult it is to weld. The problem commonly encountered in welded ASS joints is intergranular corrosion, pitting and crevice corrosion in severe corrosion environments. Weld metals of ASS may undergo precipitation of $(CrFe)_{23}C_6$ at the grain boundaries, thus depleting Cr and making the SS weldment to be preferentially susceptible to corrosion at the grain boundaries. There may also be the precipitation of the brittle sigma Fe-Cr phase in their microstructure if they are exposed to high temperatures for a certain length of time as experienced during welding. High heat input welding invariably leads to slow cooling. During this slow cooling time, the temperature range of 700 - 850^{o}C stretches in time and with it the greater formation of the sigma phase (Pickering, F.B., 1985).

In Pulsed current MPAW process, the interfuse of metals was produced by heating them with an arc using a non consumable electrode. It is widely used welding process finds applications in welding hard to weld metals such as aluminium, stainless steel, magnesium and titanium (H. B. Cary, 1989). The increased use of automated welding urges the welding procedures and selection of welding parameters must be more specific for good weld quality and precision with minimum cost (Z. Samati, 1986) . The bead geometry plays an important role in determining the microstructure of the welded specimen and the mechanical properties of the weld (P.J. Konkol and G. F. Koons,1978). The proper selection of the input welding parameters which influence the properties of welded specimen ensure a high quality joint. Stainless steels are corrosive resistance in nature finds diversified application. Even stainless posses good resistance, they are yet susceptible to pitting corrosion. The pitting corrosion is a localized dissolution of an oxide-covered metal in specific aggressive environments. It is most common and cataclysmic causes of failure of metallic structures. The detection and monitoring of pitting corrosion is an important task in determining the weld quality. The pitting corrosion is a random, sporadic and stochastic process and their prediction of the time and location of occurrence remains extremely difficult and undefined (Fong – Yuan Ma, 2012, Rao, P. S, 2004, Srinivasa Rao, P., O. P. Gupta, and S. S. N. Murty,2005).

Stainless steels may also suffer from different forms of metallurgical changes when exposed to critical temperatures. In welding, the heat affected zone often experiences temperatures which cause sufficient microstructural changes in the welded plates. The precipitation of chromium nitrides, carbides and carbonitrides in the parent metal occur under various welding and environmental conditions and also depends on the grades of stainless steel. During pulsed MPAW process, the formation of coarse grains and inter granular chromium rich carbides along the grain boundaries in the heat affected zone deteriorates the mechanical properties.

In the present paper the effect of welding parameters namely peak current, base current, pulse rate and pulse width on pitting corrosion rate of AISI 321 sheets are studied. Linear polarization method is adopted in measuring the pitting corrosion rate.

2.0 WELDING PROCEDURE

Weld specimens of 100 x 150 x 0.3mm size are prepared from AISI 321 sheets and joined using square butt joint. The chemical composition and tensile properties of AISI 321 stainless steel sheets are presented in Table .1 & 2. Argon is used as a shielding gas and a trailing gas to avoid contamination from outside atmosphere. The welding conditions adopted during welding are presented in Table .3. From the earlier works (K.Siva Prasad, Ch.Srinivasa Rao, D.Nageswara Rao, 2013,2014) carried out on Pulsed Current MPAW it was understood that the peak current, back current, pulse rate and pulse width are the dominating parameters which effect the weld quality characteristics. The values of process parameters used in this study are the optimal values obtained from our earlier papers (K.Siva Prasad, Ch.Srinivasa Rao, D.Nageswara Rao, 2013,2014). Hence peak current, back current, pulse rate and pulse width are chosen as parameters and their levels are presented in Table .4. Details about experimental setup are shown in Figure1 . Four factors and three levels are considered and according to Box-Benhken Design matrix, 27 experiments are performed as per the Design matrix shown in Table 5.

Figure 1. Micro Plasma Arc Welding Setup.

Table 1. Chemical composition of AISI 321 (weight %)

C	Si	Mn	P	S	Cr	Ni	N
0.05	0.52	1.30	0.028	0.021	17.48	9.510	0.04

Table 2. Mechanical properties of AISI 321

Elongation (%)	Yield Strength (MPa)	Ultimate Tensile Strength (Mpa)
53.20	272.15	656.30

Table 3. Welding conditions

Power source	Secheron Micro Plasma Arc Machine (Model: PLASMAFIX 50E)
Polarity	DCEN
Mode of operation	Pulse mode
Electrode	2% thoriated tungsten electrode
Electrode Diameter	1mm
Plasma gas	Argon & Hydrogen
Plasma gas flow rate	6 Lpm
Shielding gas	Argon
Shielding gas flow rate	0.4 Lpm
Purging gas	Argon
Purging gas flow rate	0.4 Lpm
Copper Nozzle diameter	1mm
Nozzle to plate distance	1mm
Welding speed	260mm/min
Torch Position	Vertical
Operation type	Automatic

Table 4. Process parameters and their limits

		Levels		
Input Factor	**Units**	**-1**	**0**	**+1**
Peak Current	Amperes	6	7	8
Base Current	Amperes	3	4	5
Pulse rate	Pulses /Second	20	40	60
Pulse width	%	30	50	70

3.0 MEASUREMENT OF PITTING CORROSION RATE

Welded joints of stainless steel are subjected to pitting corrosion when exposed to different environments. The pitting corrosion rate depends upon the type, concentration of the exposed environment and exposure time of the welded joint. The details about sample preparation and testing procedure for measurement of pitting corrosion rate are discussed in the following sections.

3.1 Surface Preparation for Plating

The welded test specimen surface is polished with 220 and 600 mesh size emery papers in the presence of distilled water continuously. The polished specimen is first rinsed with distilled water, cleaned with acetone and again rinsed with distilled water to remove the stains and grease. Finally the specimen is dried to remove the moisture content on the surface of the sample.

3.2 Sample Preparation for Corrosion studies

Once the sample is cleaned, the entire sample is covered by insulating film and only a cross sectional area of 225 mm^2 is exposed as shown in Figure 2. The perplex tube as shown in Figure 3 is attached to the test specimen.

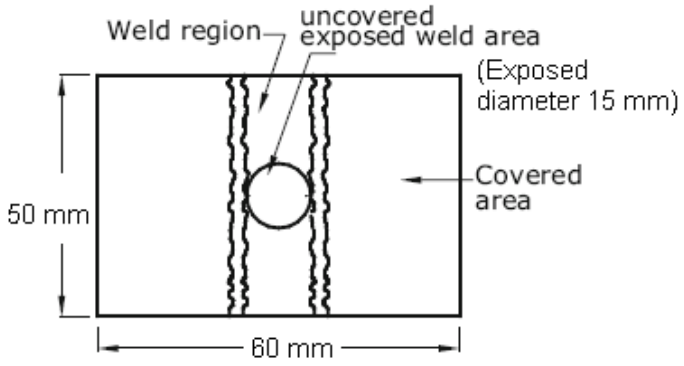

Figure 2. Dimensions of corrosion test specimen.

Figure 3. Setup of perplex tube

3.3 Procedure for Corrosion Studies

The electrochemical cell (test specimen with tube) is initially washed with distilled water followed by rinsing with filtered electrolyte NaCl. Around 100 ml of filtered electrolyte is poured into the electrochemical cell. The entire electrode assembly is now placed in the cell. The reference electrode (standard calomel electrode) is adjusted in such a way that the tip of this electrode is very near to the exposed area of working

electrode (test specimen). The auxiliary platinum electrode is also placed in the cell. Now the cell assembly has been connected to the AUTOLAB/PGSTAT12. The black colored plug has been connected to the auxiliary electrode, red colored plug to the working electrode and blue to the reference electrode. The sample has been exposed to electrolytic medium for a span of 2 hours.

As the start button of the potentiostat is switched on, the electrode potential changes continuously, till the reaction between the electrode and the medium attains equilibrium. After some time the potential remains nearly constant without any change. This steady potential which is displayed on the monitor is taken as open circuit potential (E_{rest}). Now the equipment is ready for obtaining the polarization data.

Potential is scanned cathodically until the potential is equal to E_{rest} minus the limit potential. Measurements of potential (E) and current (I) are made at different intervals and the data is displayed on the monitor itself as E vs log I plot. After reaching the cathodic limit, the scan direction is then reversed. Similarly anodic polarization data is obtained. The scan is again reversed and finally terminated and the cell is isolated from the potentiostat when the potential reached E_{rest}. The data recorded gives the Tafel plot (current vs potential data). Using the software available corrosion rate, corrosion current, polarization resistance and Tafel slopes are evaluated by Tafel plot methods. The Experimental setup is shown in Figure 4.

Figure 4. Pitting corrosion setup

3.4 Corrosion Testing Methodology

Passive metals may become susceptible to pitting corrosion when exposed to solutions having a critical content of aggressive ions such as chloride. This type of corrosion is potential-dependent and its occurrence is observed only above the pitting potential (E_{corr}), which can be used to differentiate the resistance to pitting corrosion of

differentmetal/electrolyte systems. The E_{corr} value can be determined electrochemically using both potentiostatic and potentiodynamic techniques.

3.5 Linear Polarization method

The linear polarization method utilizes the Tafel extrapolation technique. The electrochemical technique of polarization resistance is used to measure absolute corrosion rate, usually expressed in milli-inches per year (mpy), which is further converted in to mm per year. Polarization resistance can be measured very rapidly, usually less than ten minutes. Excellent correlation can often be made between corrosion rates obtained by polarization resistance and conventional weight-change determinations. Polarization resistance is also referred to as "linear polarization".

Polarization resistance measurement is performed by scanning through a potential range which is very close to the corrosion potential, E_{corr} the potential range is generally ±25 mV about E_{corr}. The resulting current vs. potential is plotted. The corrosion current, I_{corr} is related to the slope of the plot through the following equation

$$\frac{\Delta E}{\Delta I} = \frac{\beta_a \beta_c}{2.3 I_{corr}(\beta_a + \beta_c)} \quad (1)$$

where $\Delta E/\Delta I$ = slope of the polarization resistance plot, where ΔE is expressed in volts and ΔI in μA. This slope has units of resistance, hence, polarization Resistance. β_a,β_c are anode and cathode Tafel constants (must be determined from a Tafel plot as shown in Figure5).

These constants have the units of volts/decade of current. I_{corr}= corrosion current, μA. Rearranging equation (1)

$$I_{corr} = \frac{\beta_a \beta_c}{2.3(\beta_a + \beta_c)} \frac{\Delta I}{\Delta E} \quad (2)$$

The corrosion current can be related to the corrosion rate through the following equation.

$$\text{Corrosion rate (mpy)} = 0.131(I_{corr})(\text{Eq.Wt})/\rho \quad (3)$$

where

Eq.Wt = equivalent weight of the corroding species
ρ = density of the corroding species, g/cm^3
I_{corr} = corrosion current density, $\mu A/cm^2$

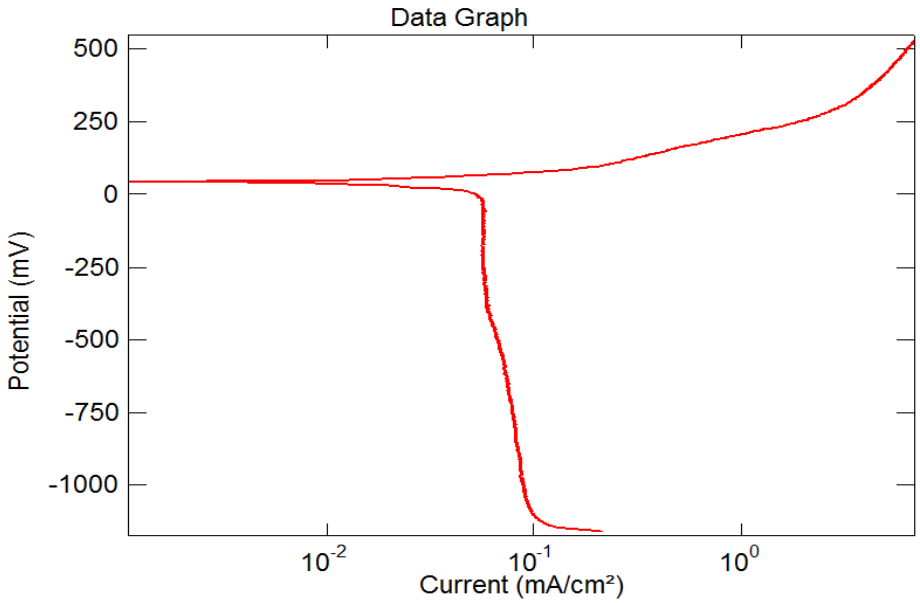

Figure 5. Modal Tafel plot

4.0 STATISTICAL ANALYSIS

The pitting corrosion rates for all the 27 samples are performed and presented in Table 5.

Table 5. Design matrix with experimental results

Experiment No.	Peak Current (Amperes)	Base current (Amperes)	Pulse Rate (Pulses/ second)	Pulse width (%)	Pitting Corrosion Rate (mm/year)	
					Experimental	Predicted
1	6	3	40	50	0.16938	0.16298
2	8	3	40	50	0.17676	0.17423
3	6	5	40	50	0.16686	0.16735
4	8	5	40	50	0.17266	0.17702
5	7	4	20	30	0.16366	0.16320
6	7	4	60	30	0.16966	0.16628
7	7	4	20	70	0.16836	0.17087
8	7	4	60	70	0.16566	0.16390
9	6	4	20	50	0.16716	0.16820
10	8	4	60	50	0.17966	0.17672
11	6	4	20	50	0.16716	0.16820
12	8	4	20	50	0.16756	0.16670
13	7	3	60	30	0.17802	0.17666
14	7	5	40	30	0.16786	0.16650
15	7	3	40	50	0.16536	0.16644
16	7	5	40	50	0.17046	0.17002
17	6	4	40	30	0.14716	0.15090

18	8	4	40	30	0.17386	0.17667
19	6	4	40	70	0.16876	0.16885
20	8	4	40	70	0.16486	0.16402
21	7	3	20	50	0.16826	0.16934
22	7	5	20	50	0.17966	0.17530
23	7	3	60	50	0.16166	0.16978
24	7	5	60	50	0.16966	0.17098
25	7	4	40	50	0.16326	0.16119
26	7	4	40	50	0.15916	0.16119
27	7	4	40	50	0.16216	0.16119

4.1 Empirical Mathematical Modeling

In RSM design, mathematical models are developed using polynomial equations. The type of polynomial equation depends on the problem.

In most RSM problems (M Balasubramanian,V Jayabalan,V Balasubramanian, 2007, 2008) the type of the relationship between the response (Y) and the independent variables is unknown. Thus the first step in RSM is to find a suitable approximation for the true functional relationship between the response and the set of independent variables.

Usually, a low order polynomial is some region of the independent variables is employed to develop a relation between the response and the independent variables. If the response is well modeled by a linear function of the independent variables then the approximating function in the first order model is

$$Y = b_o + \sum b_i x_i + \in \quad (4)$$

where b_o, $b_i$are the coefficients of the polynomial and $\in$ represents noise or error.

If interaction terms are added to main effects or first order model, then the model is capable of representing some curvature in the response function, such as

$$Y = b_o + \sum b_i x_i + \sum\sum b_{ij} x_i x_j + \in \quad (5)$$

A curve results from Equation -5 by twisting of the plane induced by the interaction term $b_{ij}x_ix_j$. There are going to be situations where the curvature in the response function is not adequately modeled by Equation -5. In such cases, a logical model to consider is

$$Y = b_o + \sum b_i x_i + \sum b_{ii} x_i^2 + \sum\sum b_{ij} x_i x_j + \in \quad (6)$$

where b_{ii} represent pure second order or quadratic effects. Equation -3 represents a second order response surface model. Using MINITAB Ver.14, statistical software, the significant coefficients are determined and final model is developed incorporating these coefficients to estimate the pitting corrosion rate. In the empirical model only significant coefficients are considered.

Pitting Corrosion Rate = $0.314280 - 0.016337X_1 - 0.059210X_2 - 0.002214X_3 + 0.001769X_4 + 0.007036X_2^2 + 0.000299X_1X_3 - 0.000382X_1X_4$

where X_1, X_2, X_3 and X_4 are the coded values of peak current, base current, pulse rate and pulse width respectively.

4.2 Checking the adequacy of the developed model for pitting corrosion rate.

The adequacy of the developed models is tested using the ANOVA. As per this technique, if the calculated value of the F_{ratio} of the developed model is less than the standard F_{ratio}(F-table value 4.60) value at a desired level of confidence of 95%, then the model is said to be adequate within the confidence limit. ANOVA test results are presented in Table 6.1 for pitting corrosion rate. From Table 6 it is understood that the developed mathematical models are found to be adequate at 95% confidence level. Coefficient of determination ' R^2' is used to find how close the predicted and experimental values lie. The value of ' R^2' for the above developed models is found to be about 0.84, which indicates a good correlation to exist between the experimental values and the predicted values. Figure6 indicate the scatter plots for pitting corrosion rate of the weld joint and reveal that the actual and predicted values are close to each other within the specified limits.

Table 6 ANOVA test results for pitting corrosion rate

Source	DF	Seq SS	Adj SS	Adj MS	F	P
Regression	14	0.000949	0.000949	0.000068	3.63	0.016
Linear	4	0.000206	0.000294	0.000074	3.94	0.029
Square	4	0.000338	0.000267	0.000067	3.57	0.039
Interaction	6	0.000404	0.000404	0.000067	3.61	0.028
Residual Error	12	0.000224	0.000224	0.000019		
Lack-of-Fit	9	0.000215	0.000215	0.000024	7.96	0.057
Pure Error	3	0.000009	0.000009	0.000003		
Total	26	0.001173				

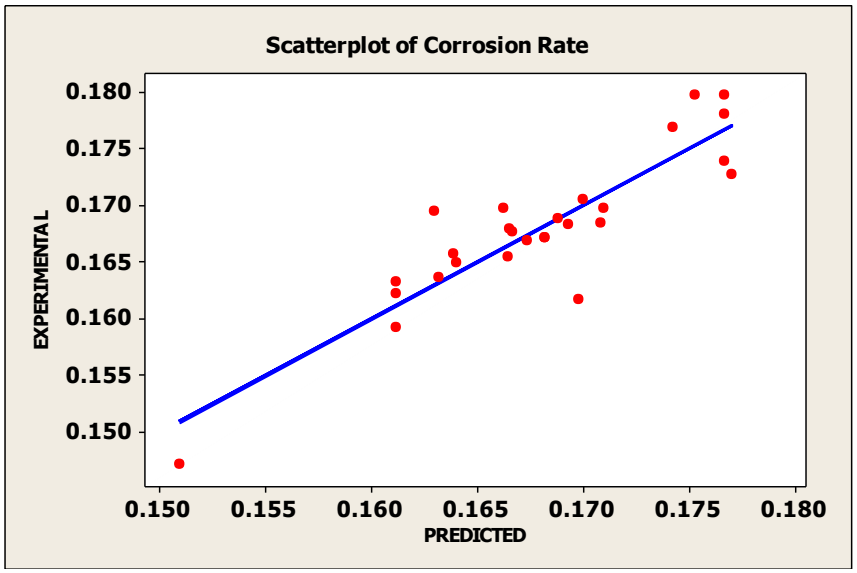

Figure 6. Scatter plot of pitting corrosion rate

5.0 RESULTS AND DISCUSSIONS

Effect of welding parameters on pitting corrosion rate is indicated by the main effect plot as shown in Figure7.

5.1 Main effect plots

From Figure 7, it is understood that the variation of each individual parameter on pitting corrosion rate can be assessed. Pitting corrosion rate increase with the peak current from 6 Amps to 8 Amps. This is because as the current increases heat input increases. At higher heat input, precipitation of $(CrFe)_{23}C_6$ at the grain boundaries takes place, thus depleting Cr and making the weldment to be preferentially susceptible to corrosion at the grain boundaries. Pitting corrosion rate decrease with the base current from 3 Amps to 4 Amps, afterwards it increases. The variation is because, at low base current generally low peak current will be used, however as the purpose of base current is to maintain the arc, instead of melting the workpice, the Pitting corrosion rate tends to decrease as precipitation of $(CrFe)_{23}C_6$ is low. But when the base current crosses over 4 Amps, corresponding peak current will increase leading to more precipitation of $(CrFe)_{23}C_6$ and hence the pitting corrosion rate increases upto 5 Amps. Pitting corrosion rate decrease with the pulse rate from 20 pulses/sec to 40 pulses/sec. This may be because, at low pulse rate, the current variation between base current and peak current is less, which leads to low heating of the base metal. However, when the pulse rate is above 40 pulses/sec, the current variation between base current and peak current is high, which leads to more melting of base metal and precipitation of $(CrFe)_{23}C_6$ at the grain boundaries. Pitting corrosion rate increase with the pulse width from 20% to 50 %. This is because as the pulse with increases, the peak current duration will be more in pulsed mode, leading to more melting and high correction rate. When the pulse width crosses

50 % , it shows a negative trend because of high time gap for cooling the base metal, which leads to lower precipitation of $(CrFe)_{23}C_6$ at the grain boundaries.

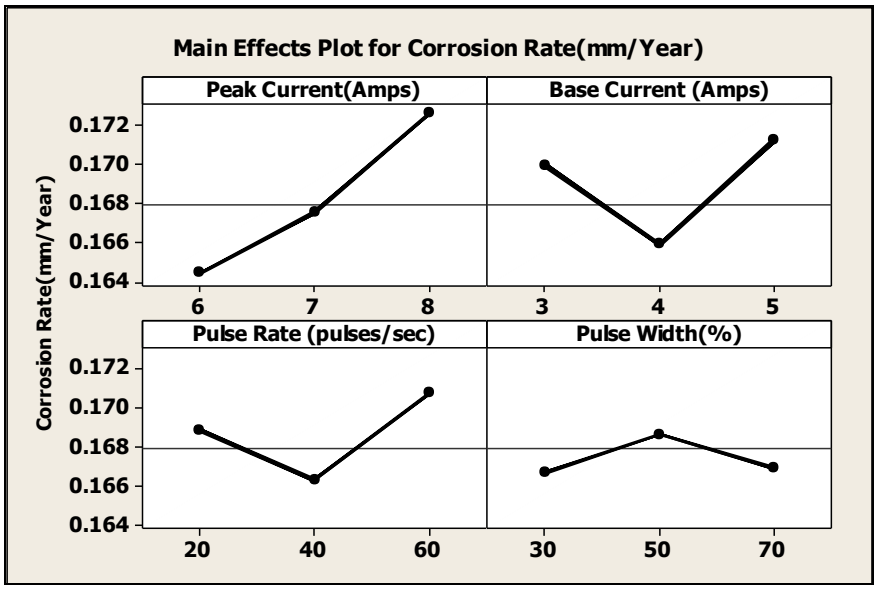

Figure 7. Main effect plot of pitting corrosion rate

5.2 Contour plots of pitting corrosion rate of 3.5N NaCl

The simultaneous effect of two parameters at a time on the output response is generally studied using contour plots and surface plots. Contour plots play a very important role in the study of the response surface. By generating contour plots using statistical software (MINITAB Ver.14) for response surface analysis, the most influencing parameter can be identified based on the orientation of contour lines. If the contour patterning of circular shaped contours occurs, it suggests the equal influence of both the factors; while elliptical contours indicate the interaction of the factors. Figure's 8a to 8f represent the contour plots for pitting corrosion rates. From these plots, the interaction effect between the input process parameters and output response can be observed as:

(i) From Figure 8a, it is understood that Pitting corrosion rate is more sensitive to change in peak current than in the base current, since the contour lines are more diverted towards peak current.

(ii) From Figure 8b, it is understood that Pitting corrosion rate is sensitive to peak current than in the pulse rate , since the contour lines are more diverted towards peak current.

(iii) From Figure 8c, it is understood that Pitting corrosion rate is more sensitive to peak current than pulse width , since the contour lines are more diverted towards peak current.

(iv) From Figure 8d, it is understood that Pitting corrosion rate is more sensitive to pulse rate than base current, since the contour lines are more diverted towards pulse rate.

(v) From Figure 8e, it is understood that Pitting corrosion rate is more sensitive to pulse width than base current , since the contour lines are more diverted towards pulse width.

(vi) From Figure 8f, it is understood that Pitting corrosion rate is more sensitive to pulse width than pulse rate , since the contour lines are more diverted towards pulse width. From the above welding parameters considered, it is understood that peak current is the most important parameter which affects the pitting corrosion rate of the welded joints.

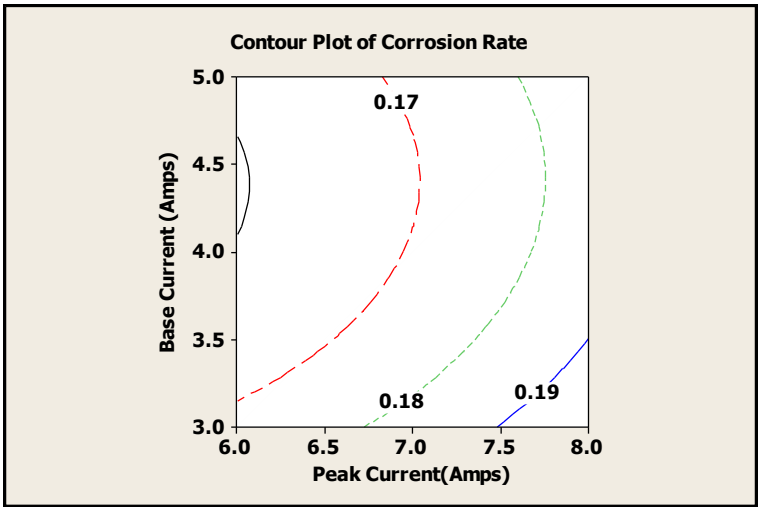

Figure 8a. Contour plot for peak current vs base current for corrosion rate (3.5N NaCl).

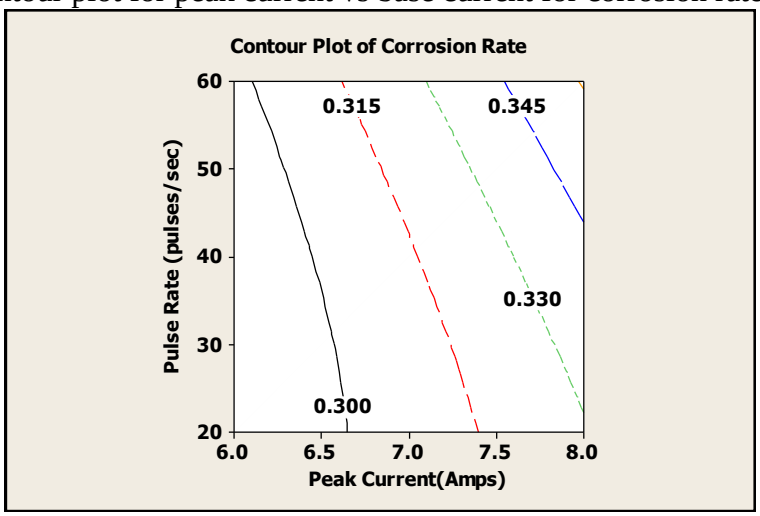

Figure 8b. Contour plot for peak current vs pulse rate for corrosion rate (3.5N NaCl).

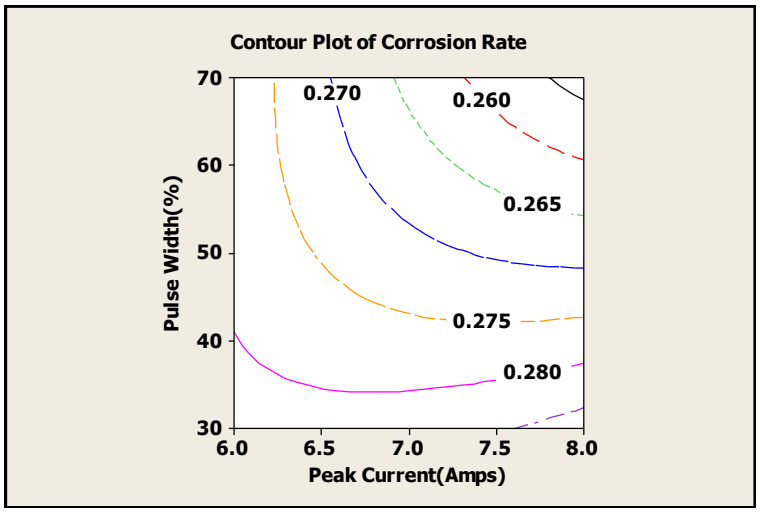

Figure 8c. Contour plot for peak current vs pulse width for corrosion rate(3.5N NaCl).

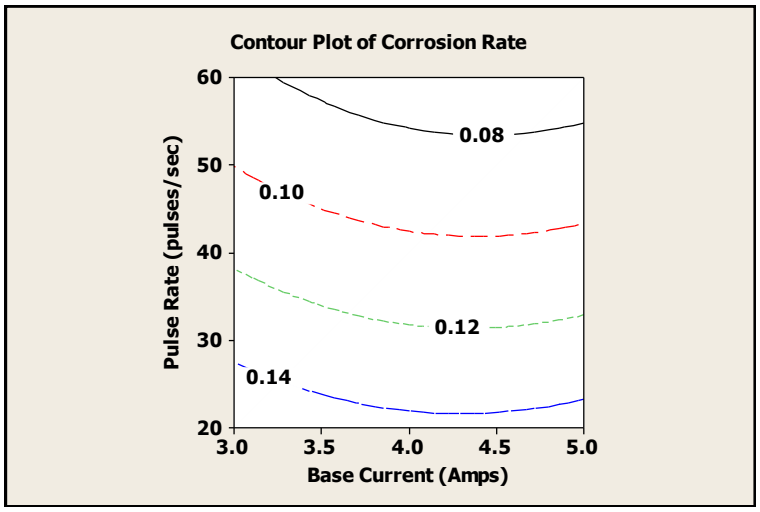

Figure 8d. Contour plot for base current vs pulse rate for corrosion (3.5N NaCl).

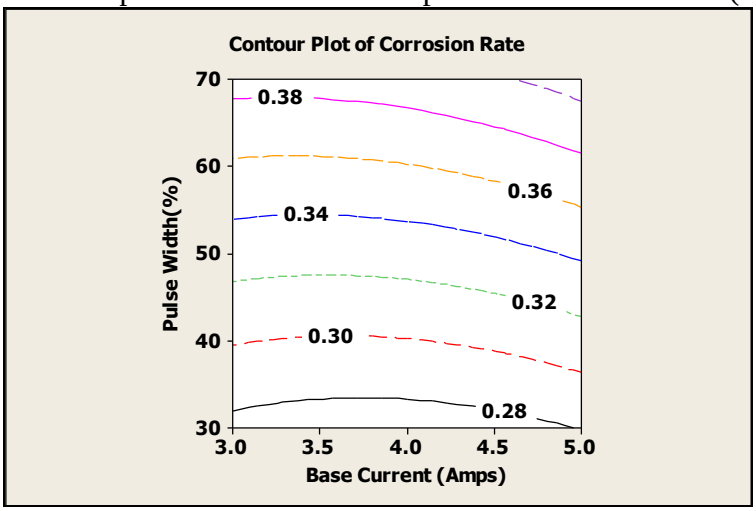

Figure 8e. Contour plot for base current vs pulse width for corrosion rate (3.5N NaCl).

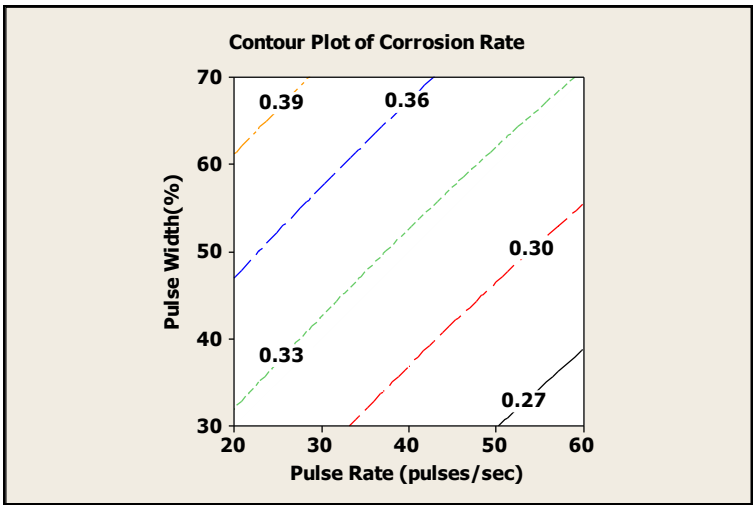

Figure 8f. Contour plot for pulse rate vs pulse width for corrosion rate (3.5N NaCl).

5.3 Surface plots

Surface plots help in locating the maximum and minimum value of the response. The maximum value of the response is represented by the apex of the surface plot, whereas the minimum value is indicated by nadir of the surface plot. The minimum pitting corrosion rate is indicated by the nadir of the response surface, as shown in Figure 9a to Figure 9f. Figure 9a the minimum pitting corrosion rate is exhibited by the nadir of the response surface. It can be seen from the twisted plane of surface plot that the model contains interaction. From the response plot, it is identified that at a peak current of 6 Amps and base current of 4 Amps, pitting corrosion rate is minimum. Figure 9b depicts that at a peak current of 6 Amps and pulse rate of 20 pulses/second, pitting corrosion rate is minimum. Figure 9c shows the three dimensional response surface plot it can be seen from the twisted plane of surface plot that the model contains interaction. From the response plot, it is identified that at the peak current of 8 Amps and pulse width of 60%, pitting corrosion rate is minimum. Figure 9d indicates that at a base current of 3 Amps and pulse rate of 60 pulses/second, pitting corrosion rate is minimum. Figure 9e represents that at a base current is 3 Amps and pulse width of 30 %, pitting corrosion rate is minimum. Figure 5.41f discusses that when pulse rate is 60 pulses/second and pulse width of 30 %, the pitting corrosion rate is minimum. It is clear from the above observations, that for a peak current of 6 Amps, base current of 3 Amps, pulse rate of 60 pulses/second and pulse width of 30 % minimum pitting corrosion rate is achieved.

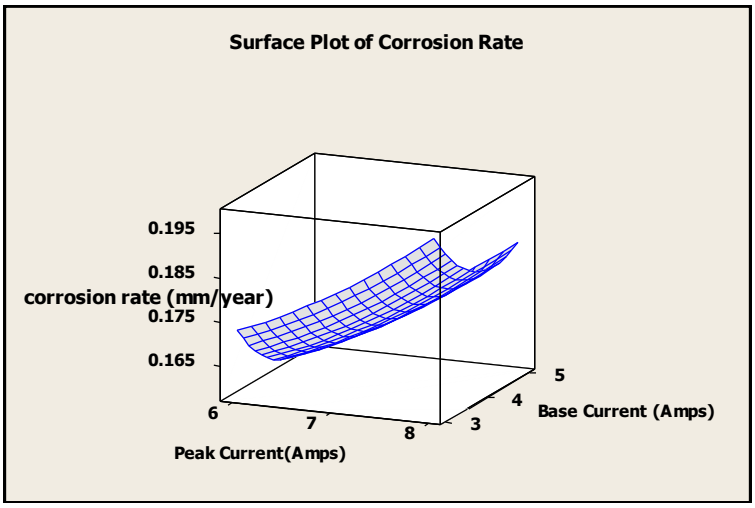

Figure 9a. Surface plot for peak current vs base current for corrosion rate (3.5N NaCl).

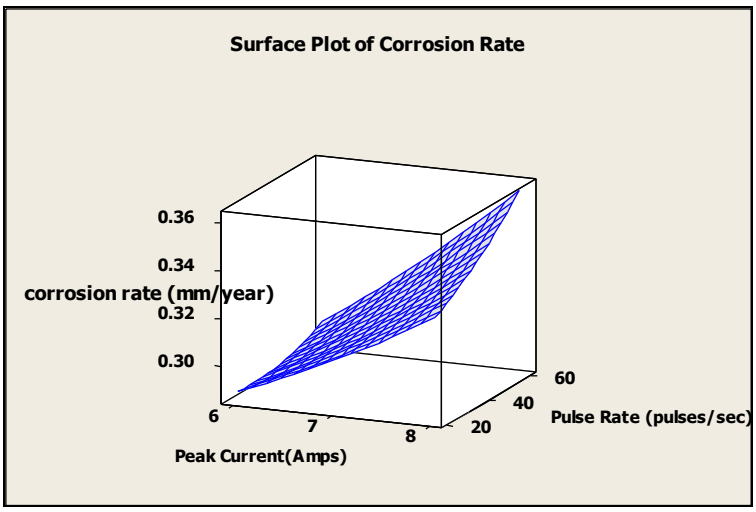

Figure 9b.Surface plot for peak current vs pulse rate for corrosion rate (3.5N NaCl).

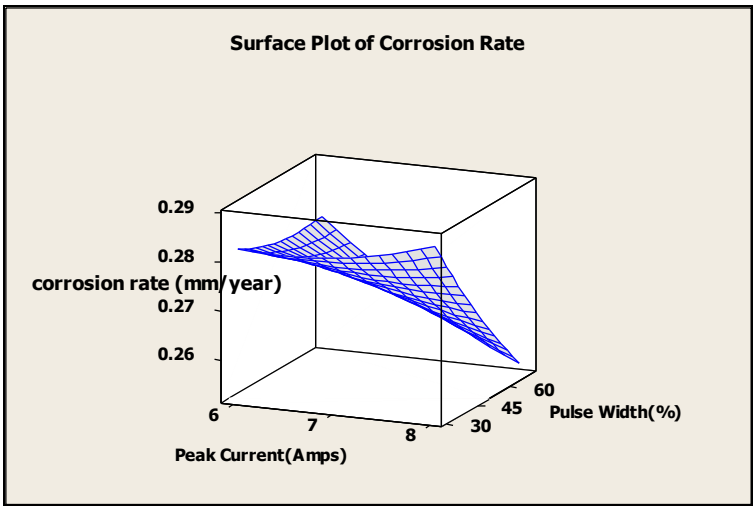

Figure 9c. Surface plot for peak current vs pulse width for corrosion rate (3.5N NaCl)

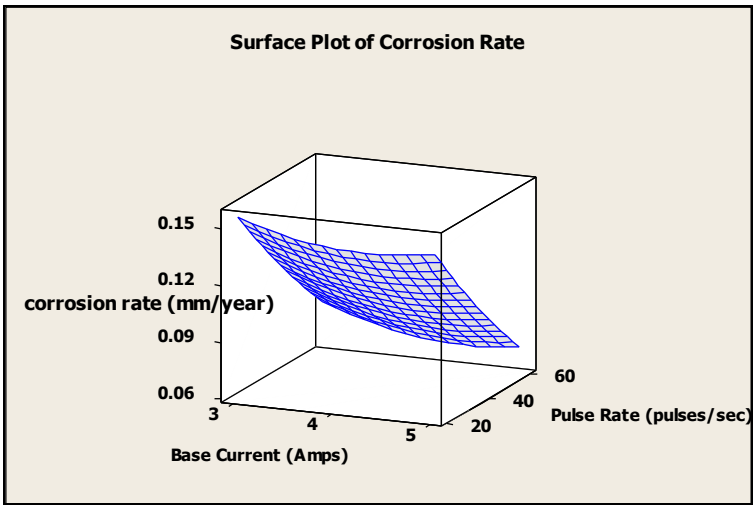

Figure 9d. Surface plot for base current vs pulse rate for corrosion rate (3.5N NaCl)

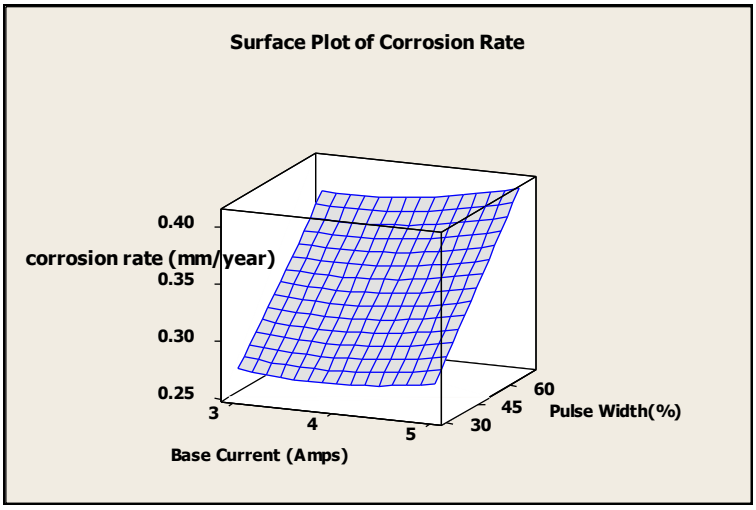

Figure 9e.Surface plot for base current vs pulse width for corrosion rate (3.5N NaCl).

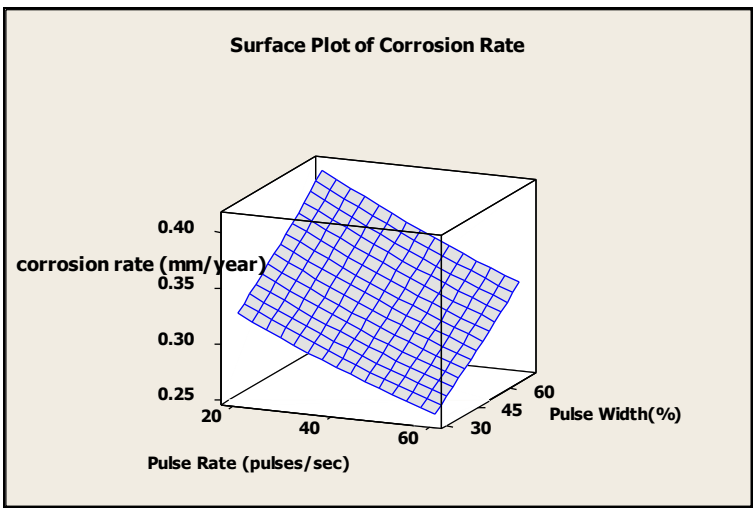

Figure 9f. Surface plot for pulse rate vs pulse width for corrosion rate (3.5N NaCl).

5.4 Microscopic analysis of weld joint

Figure 10a and 10b indicate the weld joint before corrosion and after pitting corrosion. The dark round spots indicates the area where pitting corrosion has taken place. Scanning Electron Microscope (SEM) analysis is carried out to identify the depleting of Cr % after the weld joint is subjected to pitting corrosion in 3.5N NaCl solution. Figure 11a and 11b indicate the SEM images before and after corrosion and the chemical compositions. It is observed that depletion of 3.15 % (wt.%) of Cr takes place because of corrosion.

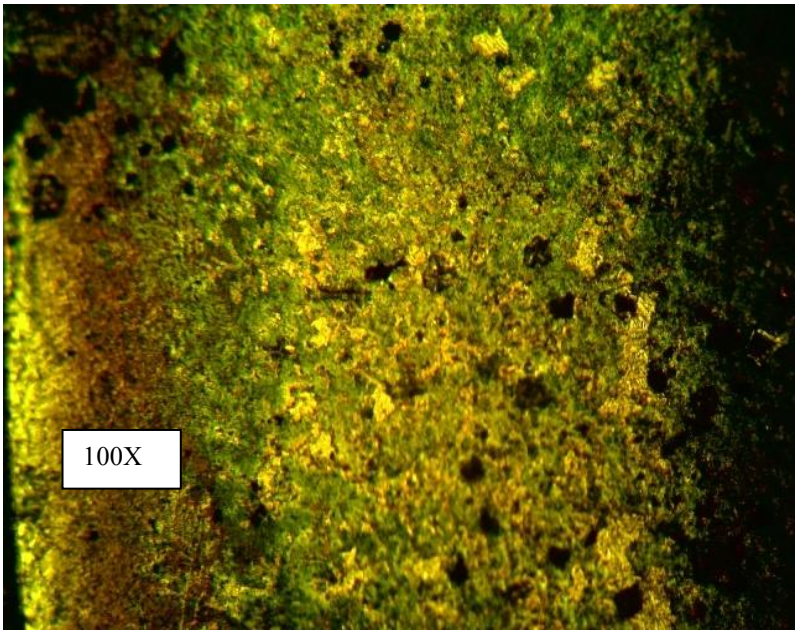

Figure.10a Weld joint before corrosion

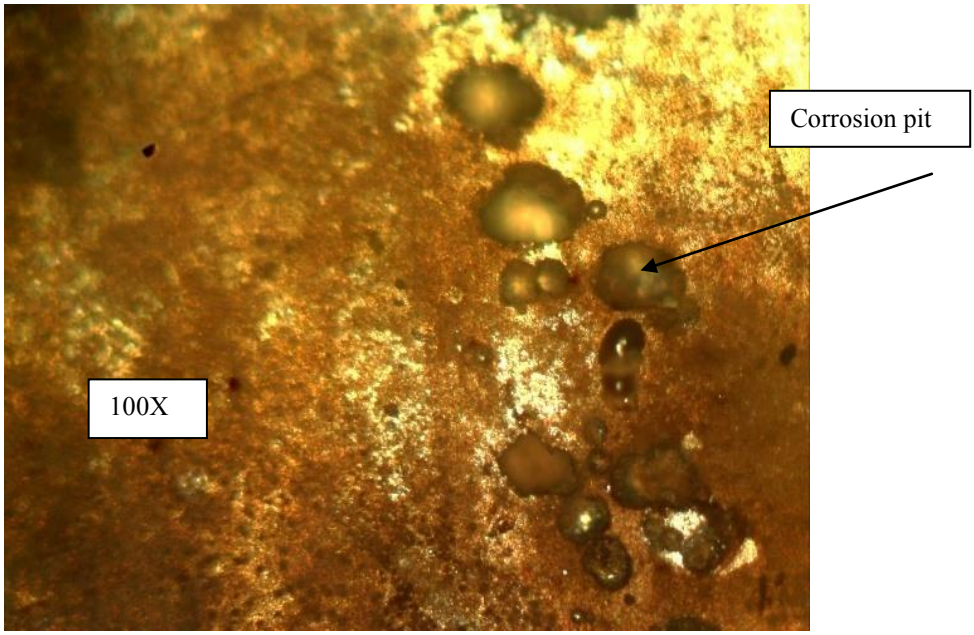

Figure.10b Weld joint after corrosion

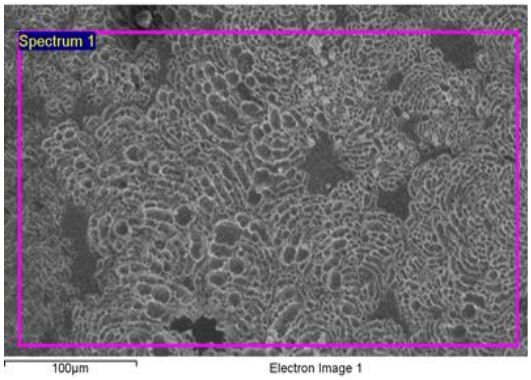

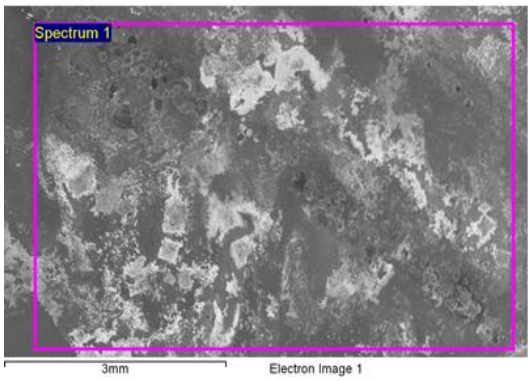

Figure11a. SEM before corrosion Figure11b. SEM after corrosion

From SEMEDAX, the chemical composition obtained of base metal and weld joint after corrosion are shown in Table7 and Table8

Table 7. Chemical compositions before corrosion

Element	O	Na	Si	Cl	Ti	Cr	Mn	Fe	Ni	Mo
Weight %	6.36	1.46	0.76	1.21	1.25	15.23	1.31	60.30	9.28	2.34
Atomic %	19.87	2.94	1.26	1.58	1.21	13.57	1.11	50.02	7.32	1.13

Table 8. Chemical compositions after corrosion

Element	O	Na	Si	Cl	Ti	Cr	Mn	Fe	Ni	Al	Cu
Weight %	12.54	16.99	0.35	8.03	0.18	12.08	0.72	42.17	5.32	0.21	0.41
Atomic %	27.04	25.49	0.43	8.79	0.13	8.01	0.45	26.04	3.12	0.27	0.22

6.0 CONCLUSIONS

The following conclusions are drawn from the experiments performed and statistical analysis. An empirical mathematical model for predicting pitting corrosion rate of pulsed current MPAW AISI 321 sheets in 3.5 N NaCl medium has been developed. From the main effect plots, it is understood that peak current is the important parameter which influences the corrosion rate, followed by base current, pulse rate and pulse width. Corrosion rate increased gradually with peak current from 6 Amps to 8 Amps, this is because of more heat input leading wider weld fusion area and higher Heat Affected Zone (HAZ). Corrosion rate decreased from Base current of 3 Amps to 4 Amps and there after it increased upto 5 Amps. This is because of variation of heat input. At 4 Amps of Base current the peak current and base current combination is optimal. Corrosion rate decreased from pulse rate of 20 pulses/sec to 40 pulses/sec and there after it increased upto 60 pulses/sec. Too low pulse rate leads to over melting of weld joint and similarly too pulse rate leads to lack of fusion. Corrosion rate increased from Pulse width of 30% to 50% and there after it decreased to 70%. Too low pulse width leads to overlapping of weld joint and similarly too high pulse width leads to lack of fusion and gaps between the weld joint. From the contour plots, it is clear that peak current is the most important parameter which affects the pitting corrosion rate of the

welded joints, followed by base current, pulse rate and pulse width. From the surface plots, it is understood that for a peak current of 6 Amps, base current of 3 Amps, pulse rate of 60 pulses/second and pulse width of 30 % minimum pitting corrosion rates are obtained for both AISI 316Ti and AISI 321. The optimal welding conditions obtained are out of the 27 combinations as per design matrix; however their values are within the range of the chosen values of welding variables. From SEMEDAX, it is observed that there is depletion of depletion of 3.15 % (wt%) chromium after corrosion was noticed in AISI 321. This is due to high heat input generated because of welding current. The developed empirical mathematical model is valid for the chosen material, however the accuracy can be improved by considering more number of factors and their levels.

7.0 REFERENCES

Dillon, C. P., (1994), *Corrosion Control in the Chemical Process Industry*, NACE International, Houston,Texas.

Fong – Yuan Ma,(2012), *Corrosive Effects of Chlorides on Metals, Pitting Corrosion*, Nasr Bensalah (Ed.),Intech open.

H. B. Cary, (1989),*Modern Welding Technology*, Prentics Hall, New Jersey.

K.Siva Prasad, Ch.Srinivasa Rao, D.Nageswara Rao,(2013), Optimization of pulsed current parameters to minimize pitting corrosion in pulsed current micro plasma arc welded AISI 304L sheets using genetic algorithm, *International Journal of Lean Thinking*, 4(1),9-19.

K.Siva Prasad, Ch.Srinivasa Rao, D.Nageswara Rao,(2013), Effect of Welding Parameters on Pitting Corrosion Rate in 3.5N NaCl of Pulsed Current Micro Plasma Arc Welded AISI 304L Sheets, *Journal of Manufacturing Science and Production*, 13(1-2),15-23.

Kondapalli Siva Prasad, Ch.Srinivasa Rao, D.Nageswara Rao,(2013), Application of Grey Relational Analysis for Optimizing Weld pool geometry parameters of Pulsed Current Micro Plasma Arc Welded AISI 304L stainless steel sheets, International *Journal of Advanced Design and Manufacturing Technology* , 6(1),pp.79-86.

Kondapalli Siva Prasad, Ch.Srinivasa Rao, D.Nageswara Rao, (2014), Multi-objective Optimization of Weld Bead Geometry Parameters of Pulsed Current Micro Plasma Arc Welded AISI 304L Stainless Steel Sheets Using Enhanced Non-dominated Sorting Genetic Algorithm, *Journal of Manufacturing science and production*, 14(2), 79-85.

M Balasubramanian, V Jayabalan, V Balasubramanian, (2007), Response Surface Approach to optimize the pulsed current gas tungsten arc welding parameters if Ti-6Al-4V titanium alloy, *Metals and Materials International*, 13(4), 335-344.

M Balasubramanian,V Jayabalan,V Balasubramanian, (2008), A mathematical model to predict impact toughness of pulsed current gas tungsten arc welded titanium alloy, *International Journal of Advanced Manufacturing Technology*, 35, 852-858.

P.J. Konkol and G. F. Koons,(1978), Optimization of Parameters for Two Wire AC-ACSAW, *American Welding Journal*, 27 , 367s – 374s.

Pickering, F.B., (1985), *Stainless Steel '84'*. The Institute of Metals: pp. 2. London.

Rao, P. S,(2004), *Development of arc rotation mechanism and experimental studies on pulsed GMA welding with and without arc rotation*, Diss. Ph. D. thesis,IIT Kharagpur.

Srinivasa Rao, P., O. P. Gupta, and S. S. N. Murty,(2005), Influence of process parameters on bead geometry in pulsed gas metal arc welding", *IIW International Congress.*

Z. Samati, (1986),*Automatic Pulsed MIG Welding*, Metal Construction, 38R- 44.